

Design of Dual-Mode Loop Resonator-Based Microwave Diplexers with Enhanced Performance

Zhe-Lin ZHU¹, Jia-Lin LI^{2,3}

¹ School of Physics, University of Electronic Science and Technology of China,
No. 2006, Xiyuan Avenue, Chengdu 611731, China

² School of Resources and Environment, University of Electronic Science and Technology of China,
No. 2006, Xiyuan Avenue, Chengdu 611731, China

³ Guangxi Key Laboratory of Wireless Wideband Communication and Signal Processing, Guilin 541004, China

zhelinzhu@std.uestc.edu.cn, jialinli@uestc.edu.cn

Submitted July 12, 2022 / Accepted September 8, 2022 / Online first October 27, 2022

Abstract. In this paper, a dual-mode loop resonator based circuit topology is studied for microwave diplexer applications. Several diplexers, with dense and sparse channel separations, are further discussed based on the introduced topology, featuring capable of controlling transmission zeros flexibly. Hence microwave diplexers with high selectivity and good channel isolation can be realized by placing transmission zeros of the channel filters at the desired channels. With the use of the proposed topology, the achieved center frequency ratio between two channels can be from 1.03 to 1.35 with good isolations, high selectivity and compact size. The demonstration diplexers are realized on PCB processes, but can be implemented with other media including MMIC. Experimental validations on the developed demonstrator are presented in the paper, and measured responses match well the full-wave electromagnetic simulated results. The developed UMTS diplexer demonstrator achieves the measured minimum passband insertion losses of 2.55 and 2.7 dB with return losses better than 15 dB and channel isolations over 40 dB at the two channels.

Keywords

Microwave diplexer, dual-mode resonator, loop resonator, microstrip resonator

1. Introduction

In modern communication systems, the microwave diplexer acts as an essential component in the RF front-ends. Generally, it is used to transmit and receive signals and is located after antennas. The frequency-division diplexer (FDD) is a filter-based circuit that separates the receiving and transmitting channels (up-links and down-links) with different operation frequencies, thus can receive and transmit signals simultaneously. Study on FDDs can be tracked back to the early 1960's [1], [2]. The FDDs usually consist of two channel filters and a T-junction network for

impedance matching. To reduce the circuitry footprint, many methods were reported. For instance, the common resonator is utilized to replace the T-junction [3–5], and the dual-mode resonators are studied in diplexer designs, where each channel corresponds to a resonant mode of a dual-mode resonance [6–9]. In addition, the defected ground structure [10], artificial electromagnetic metamaterials [11], and hybrid resonators [12] can also make the diplexer with reduced circuitry footprint. An efficient way to achieve compactness of a diplexer is to miniaturize the both channel filters.

On the other hand, a dense channel separation of a microwave diplexer can improve the spectrum utilization. However, studies show it is not easy to reduce the center frequency ratio of the two channel filters to less than 1.1 [3], [7], [8], [13]. To achieve dense channel separations, channel filters with sharp roll-off at the corners of their passbands are important. In [14], the transmission zeros and their locations of a ring-based dual-mode filter can be controlled by tuning the angle between the two excitation ports. This presents the potential to develop microwave diplexers with enhanced performance. In [15], cross-coupled open-loop resonators are developed for microstrip diplexer applications with improved channel isolations.

This paper reports our recent research on a dual-mode loop resonator with in-line feed-lines for application to the microwave diplexers. The studied diplexers with meandered loop resonator feature compact and simple topology. The dual-mode loop resonator filter with in-line feed-lines can control the transmission zeros flexibly by tuning the vertical and horizontal feeding stubs. Several microwave diplexers are discussed in this paper, including dense and sparse channel separations. The achieved frequency ratio between the two channels of the proposed diplexers can be from 1.03 to 1.35 with good performance. For demonstration purposes, a prototype diplexer with channel center frequencies of 1.95 GHz and 2.14 GHz for UMTS applications is realized and experimentally examined. Results from calculations and measurements are presented and compared, and good agreement is observed.

2. Circuit Topology and Analysis

Figure 1 shows the proposed circuit topology utilized to develop microwave diplexers in this paper. The topology consists of a pair of in-line feed-lines symmetrically and spatially separated on the resonator. A meandered loop resonator marked as nodes 1, 2, 3, 3', 4 and 5 is utilized to reduce the circuit area. The circuitry footprint is denoted as $a \times b$. The coupling between feeding stubs and the resonator is achieved using asymmetrically coupled transmission lines with coupling gaps g . The use of asymmetrically coupled transmission lines functions not only as microwave energy coupling but also as impedance transformation, which is important in building microwave filter-based diplexers. In Fig. 1, the feeding stubs along horizontal and vertical orientations are represented as c and h , respectively. With this configuration, some useful performance can be achieved, as illustrated later. It is seen from Fig. 1 that the topology is symmetric with respect to axis A-A', and therefore, the even- and odd-mode methodology is true to analyze the structure.

The first analysis is the determination of resonance frequencies. In this case, the excitation is simplified as node 1 and the perturbation stub (marked as $P_1 \times P_2$) near node 4 is formulated as a susceptance jB ($=j\omega C$, where ω is the angular frequency, and C is the equivalent capacitance of the stub). For the odd mode, axis A-A' (reference plane) is replaced by an electric wall, corresponding to a short circuit as described in Fig. 2(a). Assuming the structure is lossless and has a mean electric length θ . The odd-mode input admittance referred to node 1 can be expressed as

$$Y_{\text{odd}} = -jY \cot \theta_{1-5} - jY \cot \theta_{1-3-4} \tag{1}$$

$$= -jY (\cot \theta_{1-5} + \cot \theta_{1-3-4})$$

where Y is the characteristic admittance of the resonator, and θ_{i-j} is the electric length between nodes i and j . The odd-mode resonance can be found by imposing (1) to zero, and therefore, the odd-mode fundamental resonance frequency f_o corresponds to

$$\theta_{f_o} = 2\pi. \tag{2}$$

On the other hand, the even-mode analysis is equivalent to replacing the A-A' plane by a magnetic wall, resulting in an open circuit as depicted in Fig. 2(b). Therefore, the even-mode input admittance referred to node 1 is given by

$$Y_{\text{even}} = jY \tan \theta_{1-5} + Y \frac{j b Y + j Y \tan \theta_{1-3-4}}{Y - b Y \tan \theta_{1-3-4}} = \tag{3}$$

$$jY \frac{\tan \theta_{1-5} + \tan \theta_{1-3-4} + b - b \tan \theta_{1-5} \tan \theta_{1-3-4}}{1 - b \tan \theta_{1-3-4}}$$

where $j b$ is the normalized susceptance referred to Y , namely, $b = B/Y$. Also, the even-mode resonance is found by setting (3) to zero. For comparisons, we investigate the normalized susceptance $b = 0.01, 0.1$ and 0.5 , respectively, to find the explicit solutions. Correspondingly, the even-mode fundamental resonances frequency f_e are given by

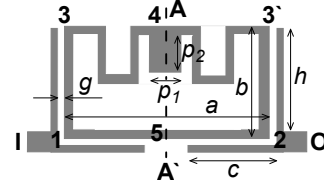


Fig. 1. Studied compact microstrip dual-mode loop resonator with input/output (I/O) excitations included.

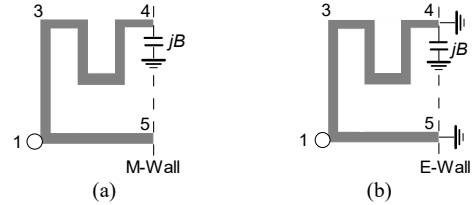


Fig. 2. Simplified equivalent networks of the resonator shown in Fig. 1, where the coupling stubs are not involved. (a) Odd mode. (b) Even mode.

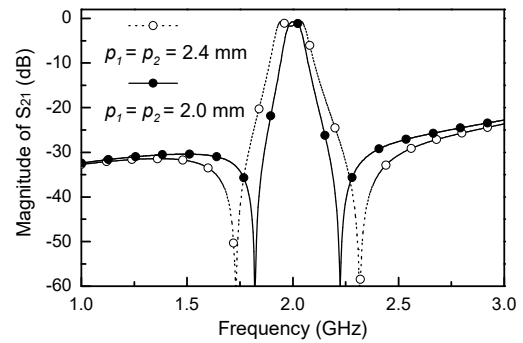


Fig. 3. Simulated frequency responses of the studied topology shown in Fig. 1, where physical parameters referred to Fig. 1 are (units: mm): $a = 14.9, b = 7.15, h = 6.95, c = 6.3, g = 0.15, w = 0.5$ and 0.45 for the resonator and feeding stub, respectively.

$$1.99\pi \quad \text{for } b = 0.01, \tag{4}$$

$$1.93\pi \quad \text{for } b = 0.10,$$

$$1.70\pi \quad \text{for } b = 0.50.$$

Based on (2) and (4), one can conclude that: 1) the fundamental odd-mode resonance corresponds to a full wavelength resonator, i.e., $\theta = 2\pi$; moreover, it is not related to the stub susceptance jB ; 2) the even-mode resonance is lower than that of the odd mode, and more importantly, it is closely associated to the stub susceptance jB . A larger stub susceptance leads to a lower even-mode fundamental resonance. This gives us a meaningful insight that the resonance space between the two modes (called as mode splitting frequency) can be controlled by varying the stub parameter in practice.

The proposed circuit structure is simulated and analyzed. The illustration circuit is studied on a dielectric substrate with a relative permittivity of 9.6 and a thickness of 0.8 mm. The simulations are carried out by using a finite element method (FEM)-based full-wave electromagnetic simulator, Ansoft Ensemble. Centered at 2.0 GHz, Figure 3 describes the simulated frequency responses of the studied circuit shown in Fig. 1. It is observed from the results that

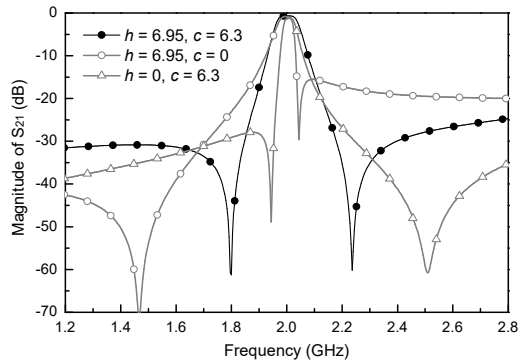


Fig. 4. Simulated responses of different couplings for the filter topology shown in Fig. 1.

the filter has a 3-dB passband bandwidth of 80 MHz when the stub size $P_1 \times P_2 = 2 \times 2 \text{ mm}^2$, and the range is changeable with the variation of $P_1 \times P_2$. Meanwhile, there are two transmission zeros clearly located near the passband, thus greatly improving the response transition between the passband and stopband. Consequently, the roll-off response is enhanced and so is the filter selectivity.

On the other hand, to achieve the high isolation for different channel separations (the up-link and down-link frequencies of a transceiver), the transmission zeros of a channel filter in FDDs should follow the channel center frequency. Therefore, the zero shifting capability of the introduced channel filter is also studied here. Shown in Fig. 4 indicates that when the horizontal stub length c varies from 6.3 to 0 mm (where $c = 6.3 \text{ mm}$ corresponds to a symmetric response as presented in Fig. 3), both transmission zeros can move to the lower frequencies (from 1.80 to 1.45 GHz and from 2.22 to 2.045 GHz, respectively). This means that reducing the horizontal coupling can shift the zeros to the lower frequency band. On the contrary, when the vertical stub varies from 6.95 to 0 mm, the vertical coupling is weakened. Results show that the zeros can be shifted respectively from 1.80 to 1.945 GHz and from 2.22 to 2.51 GHz for the lower and upper zeros. It means that the zeros are pushed to the higher frequencies under this condition. From these results, one can see that the simulation studies follow the analytical predication presented below.

3. Microwave Diplexer Based on Proposed Circuit Topology

The microwave diplexer is a three-port network as shown in Fig. 5. In general, two counterparts are involved in such a network: the channel filters (centered at f_{01} and f_{02} , respectively) and the impedance transformers. The impedance transformers present maximum energy transformation at the desired frequencies while block it at others. Therefore, at the reference plane seen in Fig. 5, the input impedance looks into the filter 1 Z_1 , should be complex conjugate the input impedance looking into the transformer 1 Z_{t1} , namely, $Z_1 = (Z_{t1})^*$, at the desired frequency band. Meanwhile, at the node N, the input impedance looks into the

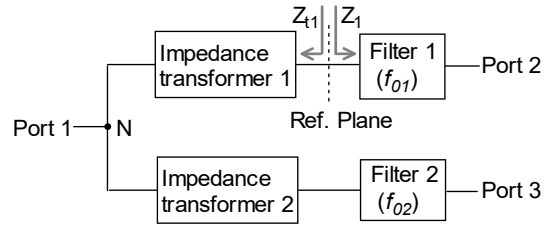


Fig. 5. General block diagram of a microwave diplexer.

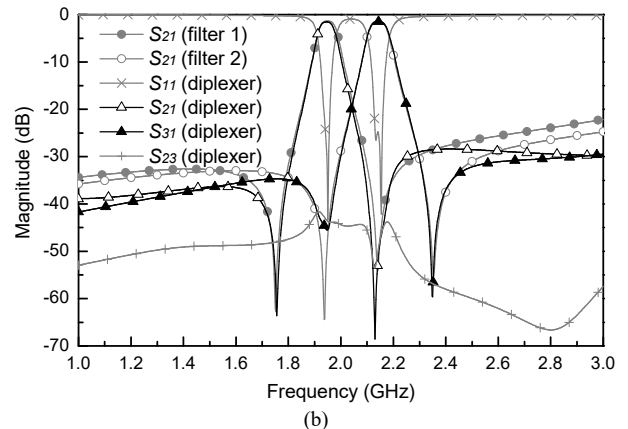
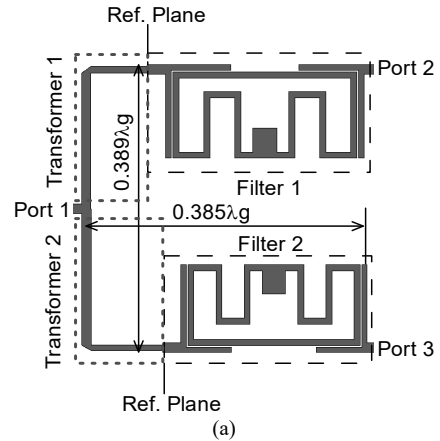


Fig. 6. (a) A diplexer (diplexer I) using the studied circuit topology. (b) Frequency responses from electromagnetic simulations.

transformer 1 should be an open circuit at the frequency f_{02} . On the other hand, $Z_1 = 0$ at f_{02} as a result of transmission zeros of the channel filter corresponding to short circuits. Hence, the transformer 1 not only performs the impedance matching at frequency f_{01} , but also functions as transition from short circuit to open circuit at frequency f_{02} . For the transformer 2, it is similar.

Several microwave diplexers are investigated here. By placing the zeros of the channel filter symmetrically with respect to its center frequency, a diplexer using the developed topology (diplexer I) is studied, where the channel center frequencies are respectively selected as 1.95 and 2.14 GHz with 3-dB bandwidths of 70 MHz for UMTS applications. Figure 6(a) shows the circuit layout. With optimal designs, it is found the circuitry footprint only occupies $0.385\lambda_g \times 0.389\lambda_g$ (where λ_g is the guided wavelength at 1.95 GHz), indicating a compact circuit size. Fig-

ure 6(b) describes the frequency responses of this diplexer. For comparisons, $|S_{21}|$ responses of the channel filters 1 and 2 are also given. It can be seen from the figure that the diplexer characterizes sharp roll-off and high selectivity. Meanwhile, a channel isolation over 40 dB is observed due to a careful placement of the transmission zeros.

Figures 7 and 8 illustrate another two diplexers using the introduced circuit topology with dense (diplexer II) and sparse (diplexer III) channel separations. By placing the transmission zeros as close as possible to the cutoff frequencies of the channel filters, results indicate that a diplexer (diplexer II) with a simple topology and very small channel separation can be realized. As shown in Fig. 7, the diplexer can operate under the channel center frequencies of 1.97 and 2.03 GHz, corresponding to a channel separation of 60 MHz, while maintaining high selectivity and high isolation. At the same time, the circuitry footprint of this diplexer is $0.436\lambda_g \times 0.378\lambda_g$. On the other hand, if the zeros are designed to be far away from the cutoff frequencies, investigations show that a diplexer (diplexer III) operation under a large channel separation can also be achieved. As depicted in Fig. 8, the diplexer having a channel separation of 600 MHz (centered at 1.70 and 2.30 GHz, respectively) can operate well. Also, high isolation and high selectivity are implemented with a simple circuit architecture and small circuitry footprint of $0.367\lambda_g \times 0.313\lambda_g$ when referred to the lower center frequency. Table 1 compares the proposed diplexers with those reported diplexers. It shows the advantages of the studied diplexers including flexible channel separations, high channel isolations, small circuitry footprint and simple topology.

Finally, the design procedure of the studied diplexer includes following two steps, given by:

Step 1: designing the channel filters based on the studied filter topology and channel center frequencies of a diplexer. For the lower channel, the upper transmission zero of the channel filter is designed to the upper channel, and vice versa.

Step 2: embedding the channel filters into a T-junction network, and by slightly tuning and optimizing the T-junction layout and parameters (the electric lengths and

Ref.	1 st /2 nd passband (GHz)	Circuitry footprint (λ_g^2)	Isolations (dB)	In-band ILs & RLs (dB)	Frequency ratio
[3]	1.95/2.14	0.53×0.31	> 36	1.46, 1.44, > 12	1.1
[4]	1.50/1.76	0.50×0.33	> 30	2.8, 3.2, > 16	1.17
[7]	1.95/2.14	0.36×0.38	> 35	1.2, 1.5, > 12	1.1
[8]	1.75/1.85	0.47×0.15	> 20	2.1, 2.1, 20	1.06
[15]	1.77/1.93	1.53×0.43	> 50	2.88, 2.95, > 18	1.09
This work	1.95/2.14	0.38×0.40	> 42	2.55, 2.7, > 15	1.1
	1.97/2.03	0.44×0.38	> 35	1.5, 1.5, > 20*	1.03
	1.70/2.30	0.37×0.31	> 42	1.5, 1.5, > 20*	1.35

IL: insertion loss; RL: return loss; * denotes simulated results.

Tab. 1. Comparisons between the proposed diplexer and some reported results.

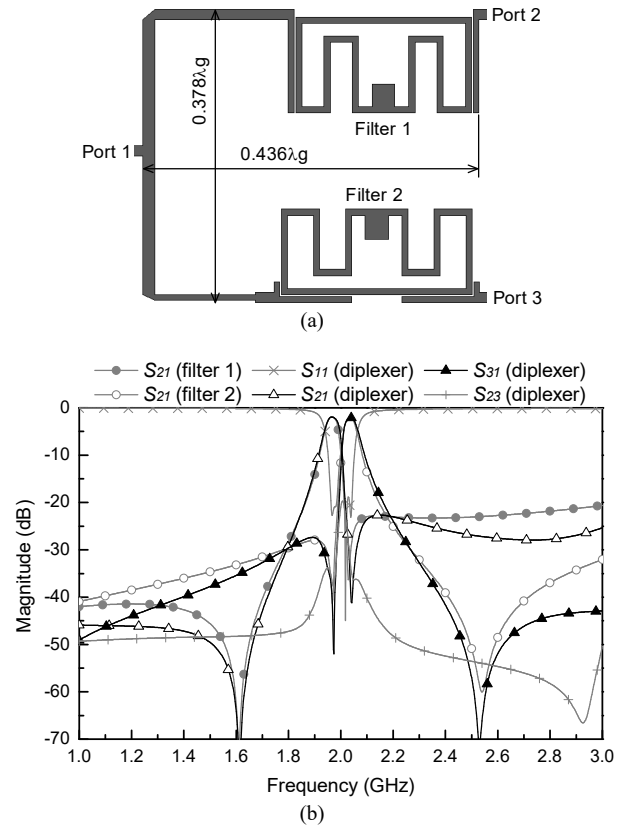


Fig. 7. (a) Layout of a diplexer with dense channel separation (diplexer II). (b) Performance from simulations.

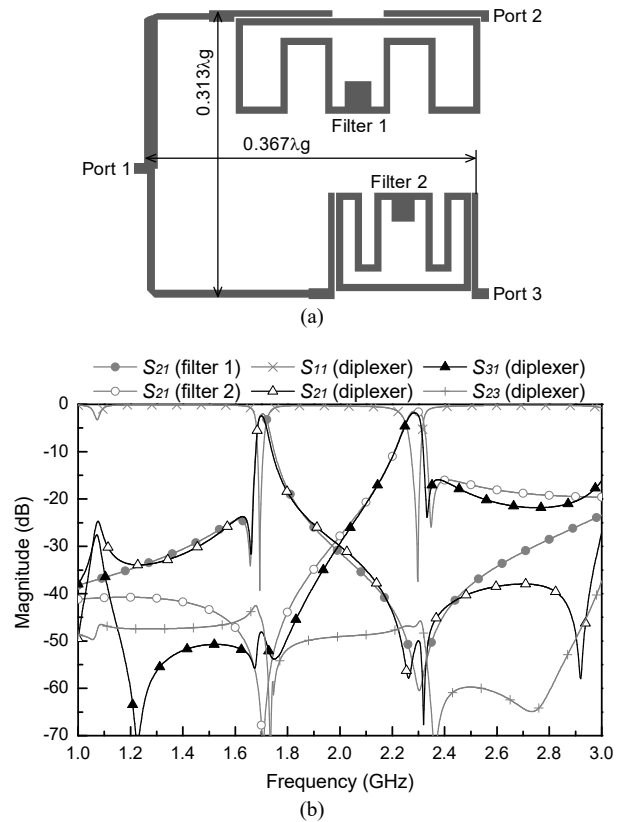


Fig. 8. (a) Layout of a diplexer with sparse channel separation (diplexer III). (b) Simulated frequency responses.

characteristic impedances of the two transformers as sketched in Fig. 5) to achieve the desired responses.

4. Demonstration on Microwave Diplexer using Studied Topology

To confirm the investigations, a demonstrator diplexer circuit based on diplexer I is built on a microwave dielectric substrate mentioned above. Figure 9 is a photograph of the fabricated circuit. The measurements are carried out using an HP 8753ES network analyzer together with through-reflect-line (TRL) calibrations. All measured responses and simulated results are described in Fig. 10. It is found from experiments that the measured center frequencies of the two channels are 1.95 and 2.16 GHz with minimum passband insertion losses ($|S_{21}|$ and $|S_{31}|$) being 2.55 and 2.7 dB, respectively. Meanwhile, isolations better than 40 dB at the two channels are observed, validating the high isolation experimentally. As compared to the measurements and predicated results shown in Fig. 10(a), good agreement can be found. On the other hand, the measured group delays are approximately 5 ns at the two channels, as presented in Fig. 10(b).

5. Conclusion

A microstrip loop resonator with meandered topology and in-line feed line has been studied in this paper. With simple circuit layout and controllable response zeros, the introduced topology is interesting to be found in application to the microwave diplexers with high channel selectivity, sharp roll-off and high isolation as well as compact size. Several diplexers have been investigated and confirmed from simulations. For demonstration purposes, one of them for the UMTS application has been designed, built and examined experimentally. The results show good agreement between the predications and measurements. The developed demonstrator features the measured minimum passband insertion losses of 2.55 and 2.7 dB with the return losses better than 15 dB and channel isolations over 40 dB at the two channels. Meanwhile, the circuitry footprint is $0.38 \times 0.40 \lambda_g^2$. It is believed that the developed diplexers are attractive for further integration into the microwave communication transceivers in today's wireless systems, where stringent system requirements such as volume, weight, power, cost and so on are suffered from.

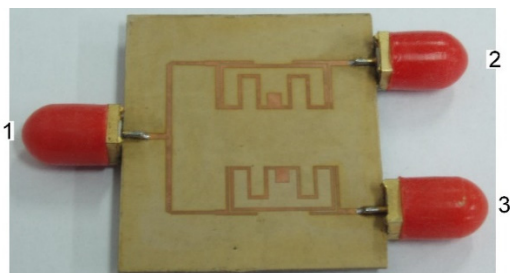


Fig. 9. Photograph of the developed diplexer.

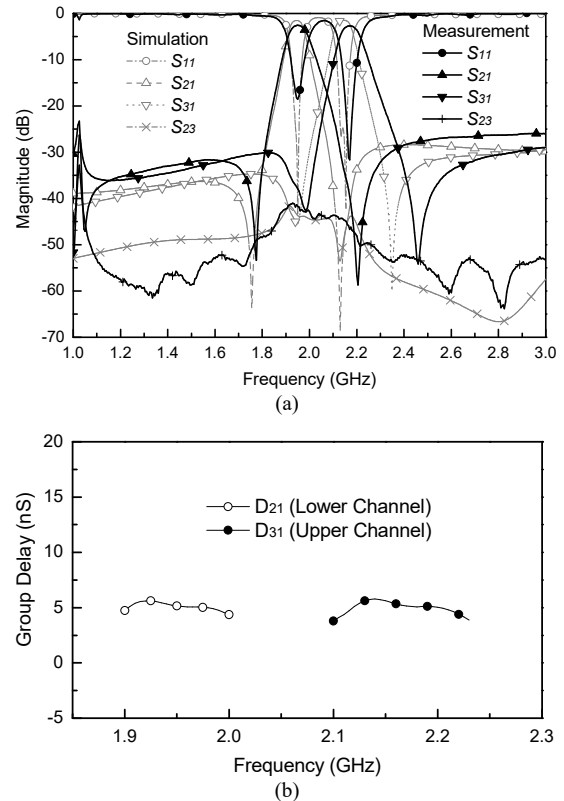


Fig. 10. Performance of the studied diplexer I. (a) Return loss, insertion loss and isolation responses. (b) Group delays from experimental examinations.

Acknowledgement

This work was supported in part by the Natural Science Foundation of China (NSFC) under grant No. 62271105, and in part by the Guangxi Key Laboratory of Wireless Wideband Communication and Signal Processing under grant No. GXKL06220205, Guilin University of Electronic Technology, China.

References

- [1] MATTHAEI, G. L., CRISTAL, E. G. Multiplexer channel-separating units using interdigital and parallel-coupled filters. *IEEE Transactions on Microwave Theory and Techniques*, 1965, vol. 13, no. 3, p. 328–334. DOI: 10.1109/TMTT.1965.1125997
- [2] WENZEL, R. J. Printed-circuit complementary filters for narrow bandwidth multiplexers. *IEEE Transactions on Microwave Theory and Techniques*, 1968, vol. 16, no. 3, p. 147–157. DOI: 10.1109/TMTT.1968.1126635
- [3] CHUANG, M. L., WU, M. T. Microstrip diplexer design using common T-shaped resonator. *IEEE Microwave and Wireless Components Letters*, 2011, vol. 21, no. 11, p. 583–585. DOI: 10.1109/LMWC.2011.2168949
- [4] CHEN, C. F., HUANG, T. Y., CHOU, C. P., et al. Microstrip diplexers design with common resonator sections for compact size, but high isolation. *IEEE Transactions on Microwave Theory and Techniques*, 2006, vol. 54, no. 5, p. 1945–1952. DOI: 10.1109/TMTT.2006.873613

- [5] TANTIVIWAT, S., INTARAWISET, N., JEENAWONG, R. Wide-stopband, compact microstrip diplexer with common resonator using stepped-impedance resonators. In *1st IEEE Tencon Spring Conference for Region 10*. Sydney (Australia), 2013, p. 174–177. DOI: 10.1109/TENCONSpring.2013.6584435
- [6] CHEN, D., ZHU, L., BU, H., et al. A novel planar diplexer using slotline-loaded microstrip ring resonator. *IEEE Microwave and Wireless Components Letters*, 2015, vol. 25, no. 11, p. 706–708. DOI: 10.1109/LMWC.2015.2479836
- [7] GUAN, X., YANG, F., LIU, H., et al. Compact and high-isolation diplexer using dual-mode stub-loaded resonators. *IEEE Microwave and Wireless Components Letters*, 2014, vol. 24, no. 6, p. 385 to 387. DOI: 10.1109/LMWC.2014.2313591
- [8] PENG, H. S., CHIANG, Y. C. Microstrip diplexer constructed with new types of dual-mode ring filters. *IEEE Microwave and Wireless Components Letters*, 2015, vol. 25, no. 1, p. 7–9. DOI: 10.1109/LMWC.2014.2365740
- [9] SONG, K., YAN, Y., ZHONG, C., et al. Compact multimode-resonator diplexer with wide upper-stopband and high isolation. *Electromagnetics*, 2019, vol. 39, no. 4, p. 262–270. DOI: 10.1080/02726343.2019.1595387
- [10] SONG, K., ZHOU, Y., CHEN, Y., et al. Compact high-isolation multiplexer with wide stopband using spiral defected ground resonator. *IEEE Access*, 2019, vol. 7, p. 31702–31710. DOI: 10.1109/ACCESS.2019.2901794
- [11] DONG, Y., ITOH, T. Substrate integrated waveguide loaded by complementary split-ring resonators for miniaturized diplexer design. *IEEE Microwave and Wireless Components Letters*, 2011, vol. 21, no. 1, p. 10–12. DOI: 10.1109/LMWC.2010.2091263
- [12] YANG, T., CHI, P. L., ITOH, T. High isolation and compact diplexer using the hybrid resonators. *IEEE Microwave and Wireless Components Letters*, 2010, vol. 20, no. 10, p. 551–553. DOI: 10.1109/LMWC.2010.2052793
- [13] GORUR, A. K., TURKELI, A., DOGAN, E., et al. A novel compact microstrip diplexer with closely spaced channels. In *50th European Microwave Conference*. Utrecht (The Netherlands), 2020, p. 116–119. DOI: 10.23919/EuMC48046.2021.9338170
- [14] LUO, S., ZHU, L., SUN, S. A dual-band ring-resonator bandpass filter based on two pairs of degenerate modes. *IEEE Transactions on Microwave Theory and Techniques*, 2010, vol. 58, no. 12, p. 3427–3432. DOI: 10.1109/TMTT.2010.2053590
- [15] NWAJANA, A. O., YEO, K. S. K. Microwave diplexer purely based on direct synchronous and asynchronous coupling. *Radioengineering*, 2016, vol. 25, no. 2, p. 247–252. DOI: 10.13164/re.2016.0247

About the Authors ...

Zhe-Lin ZHU was born in 1999. He is currently pursuing master's degree in the School of Physics, University of Electronic Science and Technology of China, Chengdu, China. His research interests include microwave/millimeter-wave antennas and arrays.

Jia-Lin LI received the M. S. degree from the University of Electronic Science and Technology of China (UESTC), Chengdu, China, in 2004, and the Ph. D. degree from the City University of Hong Kong, Hong Kong, in 2009, both in Electronic Engineering. From September 2005 to August 2006, he was a Research Associate with the Wireless Communication Research Center, City University of Hong Kong, Hong Kong. From September 2009 to April 2021, he was a Lecturer first and then a Professor with the School of Physical Electronics, UESTC. From May 2021 to now, he has been with the School of Resources and Environment, UESTC, as a Professor. His research interests include microwave/millimeter-wave antennas and arrays, circuits and systems, and so on.